

Stacking-velocity inversion with borehole constraints for tilted TI media

Xiaoxiang Wang¹ and Ilya Tsvankin¹

ABSTRACT

Transversely isotropic models with a tilted symmetry axis (TTI) play an increasingly important role in seismic imaging, especially near salt bodies and in active tectonic areas. Here, we present a 2D parameter-estimation methodology for TTI media based on combining P-wave normal-moveout (NMO) velocities, zero-offset traveltimes, and reflection time slopes with borehole data that include check-shot traveltimes as well as the reflector depths and dips. For a dipping TTI layer with the symmetry axis confined to the dip plane of the reflector, simultaneous estimation of the symmetry-direction velocity V_{p0} , the anisotropy parameters ϵ and δ , and the tilt ν of the symmetry axis proves to be ambiguous despite the borehole constraints. If the symmetry axis is orthogonal to the reflector, V_{p0} and δ can be recovered with high accuracy, even when the symmetry axis deviates by $\pm 5^\circ$ from the reflector normal. The parameter ϵ , however, cannot be constrained for dips smaller than 60° without using nonhyperbolic moveout. To invert for the interval parameters of layered TTI media, we apply 2D stacking-velocity inversion supplemented with the same borehole constraints. The dip planes in all layers are assumed to be aligned, and the symmetry axis is set orthogonal to the reflector in each layer. Information about reflector dips can be replaced with near-offset walkaway vertical seismic profiling (VSP) traveltimes. Tests on noise-contaminated data demonstrate that the algorithm produces stable estimates of the interval parameters V_{p0} and δ , if the range of dips does not exceed 30° . Our method can be used to build an accurate initial TTI model for post-migration reflection tomography and other techniques that employ migration velocity analysis.

INTRODUCTION

Ignoring anisotropy in P-wave processing causes imaging and interpretation errors, such as mispositioning of horizontal and dipping

reflectors (e.g., Alkhalifah and Larner, 1994; Alkhalifah et al., 1996; Vestrum et al., 1999). While many widely used migration algorithms have been extended to transversely isotropic (TI) media, constructing an accurate anisotropic velocity model remains a challenging problem. For TI models with a vertical symmetry axis (VTI), the depth-domain P-wave velocity field is controlled by the vertical velocity V_{p0} and the Thomsen (1986) parameters ϵ and δ . To resolve all three parameters individually, P-wave moveout typically has to be combined with borehole data or shear modes (SS- or PS-waves) (Sexton and Williamson, 1998; Tsvankin and Grechka, 2000).

Vertical transverse isotropy has proved to be adequate for most horizontally stratified, unfractured sediments. However, in progradational clastic or carbonate sequences, as well as in the presence of obliquely dipping fractures, the symmetry axis is tilted (Figure 1). Also, transverse isotropy with a tilted symmetry axis (TTI) is an appropriate model for dipping shale layers near salt domes and in fold-and-thrust belts such as the Canadian Foothills (Isaac and Lawton, 1999; Vestrum et al., 1999; Charles et al., 2008; Huang et al., 2008; Behera and Tsvankin, 2009). The parameters V_{p0} , ϵ , and δ for TTI media are defined in the rotated coordinate system with respect to the symmetry axis, whose orientation is described by the tilt angle ν with the vertical and the azimuth β .

In principle, the symmetry-axis orientation and the interval parameters V_{p0} , ϵ , and δ of a TTI layer can be estimated from wide-azimuth P-wave data (Grechka and Tsvankin, 2000), if the medium is not close to elliptical (i.e., $\epsilon \neq \delta$). Stable inversion, however, requires at least two NMO ellipses from interfaces with different orientations (e.g., a horizontal and a dipping reflector). Also the tilt ν of the symmetry axis has to exceed 30° and the reflector dip ϕ should be between 30° and 80° (Grechka and Tsvankin, 2000). If shear data are available, the addition of the SV-wave NMO ellipse from a horizontal reflector helps increase the inversion accuracy and makes parameter estimation possible for elliptically anisotropic media. Still, combining horizontal SV-wave events with P-wave data does not remove the above constraints on ν and ϕ (Grechka and Tsvankin, 2000).

Grechka et al. (2002a) develop a multicomponent inversion algorithm for interval parameter estimation in layered TI media using wide-azimuth PP and PS (or SS) reflection data. For relatively large

Manuscript received by the Editor 18 December 2009; revised manuscript received 9 March 2010; published online 6 October 2010.
¹Colorado School of Mines, Department of Geophysics, Center for Wave Phenomena. E-mail: xwang@mines.edu; ilya@dix.mines.edu.
© 2010 Society of Exploration Geophysicists. All rights reserved.

tilt angles ν and reflector dips, multicomponent, multi-azimuth reflection data can be used to build anisotropic models for depth processing. However, parameter estimation is still ambiguous for a wide range of small and moderate angles ν and ϕ (Figure 2), mainly because of the multimodal nature of the misfit function.

To carry out parameter estimation for a horizontal TTI layer, Dewangan and Tsvankin (2006a) apply the PP + PS = SS method (Grechka and Tsvankin, 2002b; Grechka and Dewangan, 2003) to reflection traveltimes of PP- and PS-waves. They implement nonlinear inversion of the NMO velocities and zero-offset traveltimes of the recorded PP-waves and computed SS-waves combined with the moveout-asymmetry attributes of the PS(PSV)-waves.² The method of Dewangan and Tsvankin (2006a) remains accurate for a wide range of tilts, except for “quasi-VTI” models with $\nu < 10^\circ$.

In a sequel paper, Dewangan and Tsvankin (2006b) extend this al-

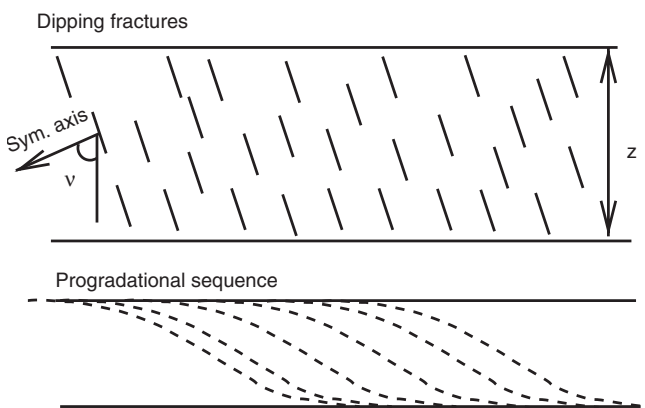


Figure 1. TI layer with a tilted symmetry axis may describe progradational sequences and a system of obliquely dipping, penny-shaped fractures embedded in isotropic host rock (after Dewangan and Tsvankin, 2006a).

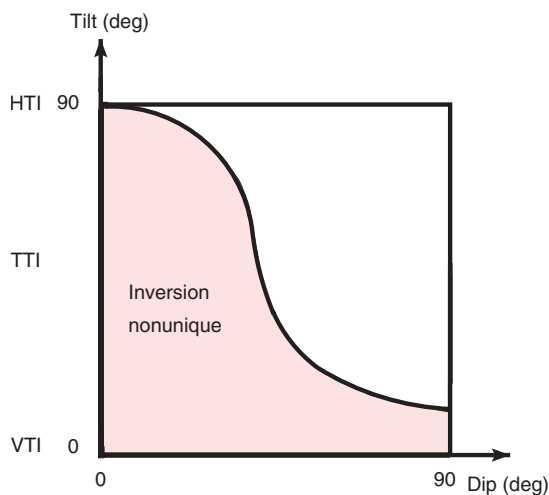


Figure 2. Illustration of the uniqueness of depth-domain parameter estimation for TI media using wide-azimuth, multicomponent data (after Grechka et al., 2002a). The tilt and azimuth of the symmetry axis are assumed to be unknown, even for VTI and HTI models.

²The moveout of PS-waves is asymmetric if the traveltime does not stay the same when the source and receiver are interchanged. In a horizontal TTI layer, this asymmetry is caused by the tilt of the symmetry axis.

gorithm to a dipping TTI layer with the symmetry axis orthogonal to the layer’s bottom. In that model, the moveout asymmetry of PS-waves is caused not just by the tilted symmetry axis, but also by the reflector dip. Despite the fixed axis orientation, parameter estimation is stable only for significant tilts ($\nu > 30^\circ - 40^\circ$), with the anisotropy parameter δ constrained more tightly than ϵ .

Although PS-waves provide valuable information for velocity model building in the depth domain, they are not routinely acquired in exploration. Also, processing of mode-converted data is much more difficult than that of pure PP reflections due to such inherent features of PS-waves as the raypath and moveout asymmetry, polarity reversals, and low amplitudes at small offsets. Also, it is often challenging to identify PP and PS events from the same interface because of their different reflectivities and of the depth-varying V_P/V_S ratio.

Here, we present a 2D inversion methodology for a stack of homogeneous TTI layers based on combining conventional-spread P-wave moveout with borehole information. P-wave NMO velocities, reflection slopes, and zero-offset traveltimes are supplemented with check-shot traveltimes and reflector depths and dips. First, we introduce a semi-analytic inversion procedure for a single TTI layer above a dipping interface and show that the medium parameters cannot be resolved without constraining the tilt of the symmetry axis. Then we develop joint inversion of moveout and borehole data for a stack of TTI layers with the symmetry axis orthogonal to the lower boundary of each layer. Whereas the reflector depths have to be known, dip information can be replaced with VSP traveltimes for nonzero offsets. Synthetic tests with a realistic level of Gaussian noise illustrate the stability of estimating the interval parameters V_{P0} , ϵ , and δ .

INVERSION FOR A SINGLE TTI LAYER

We start by considering the simple model of a homogeneous TTI layer above a plane dipping reflector. To make the problem 2D, the symmetry axis is assumed to be confined to the dip plane (Figure 3). The tilt angle ν is taken positive, if the symmetry axis is rotated counterclockwise from the vertical. P-wave surface data provide the zero-offset reflection time t_0 , the reflection slope (horizontal slowness) p on the zero-offset time section, and the NMO velocity V_{nmo} . Because the layer is homogeneous, t_0 , p , and V_{nmo} can be estimated

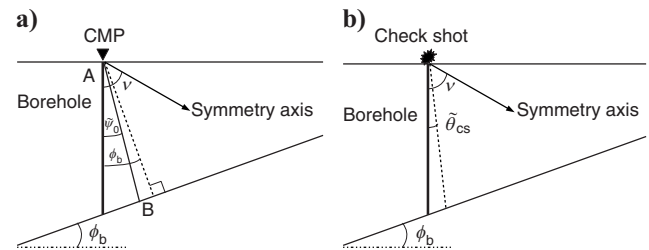


Figure 3. Dipping TTI layer with the CMP at the head of a vertical borehole. The arrow marks the symmetry axis; the reflector dip is ϕ_b . (a) AB is the zero-offset raypath; the phase and group angles of the zero-offset ray with the vertical are ϕ_b and ψ_0 , respectively. (b) The phase-velocity vector of the vertical (check-shot) ray makes the angle θ_{cs} with the vertical.

for a single common midpoint (CMP). It is assumed that the depth and dip of the reflector are measured at a borehole location along with the P-wave group velocity obtained from check shots.

Arbitrary axis orientation

Inversion methodology

The exact P-wave phase-velocity function in TI media expressed through the Thomsen parameters is given by (Tsvankin, 1996, 2005)

$$\frac{V^2}{V_{P0}^2} = 1 + \epsilon \sin^2 \theta - \frac{f}{2} + \frac{f}{2} \sqrt{1 + \frac{4\sin^2 \theta}{f} (2\delta \cos^2 \theta - \epsilon \cos 2\theta) + \frac{4\epsilon^2 \sin^4 \theta}{f^2}}, \quad (1)$$

where θ is the phase angle with the symmetry axis (assumed to be positive for counterclockwise rotation), V_{P0} is the symmetry-direction velocity, and

$$f \equiv 1 - \frac{V_{S0}^2}{V_{P0}^2}, \quad (2)$$

V_{S0} is the symmetry-direction velocity of S-waves. Because the influence of V_{S0} on P-wave kinematics is negligible, the value of f can be set to a constant using a typical V_{P0}/V_{S0} ratio (e.g., $V_{P0}/V_{S0} = 2$). Therefore, the phase velocity V represents a function of four medium parameters (V_{P0} , ϵ , δ , and ν) and the phase angle $\tilde{\theta}$ with the vertical:

$$V = f_1(V_{P0}, \epsilon, \delta, \theta) = f_1(V_{P0}, \epsilon, \delta, \tilde{\theta}, \nu), \quad (3)$$

where $\theta = \tilde{\theta} - \nu$.

For the zero-offset reflection, the phase-velocity (slowness) vector is perpendicular to the reflector, and the phase angle with the vertical $\tilde{\theta}$ is equal to the dip ϕ_b (Figure 3a; the subscript “b” denotes borehole data). The phase velocity for the zero-offset reflection can be computed through the known values of ϕ_b and p as

$$V_{\phi_b} = \frac{\sin \phi_b}{p}. \quad (4)$$

Substituting equation 4 into equation 3 yields

$$f_1(V_{P0}, \epsilon, \delta, \phi_b, \nu) = \frac{\sin \phi_b}{p}. \quad (5)$$

The P-wave group velocity V_G in TI media can be found as a function of the phase velocity V and its derivative with respect to θ (e.g., Tsvankin, 2005):

$$V_G = V \sqrt{1 + \left(\frac{1}{V} \frac{dV}{d\theta} \right)^2}. \quad (6)$$

Therefore, V_G represents a function (different from f_1) of the parameters V_{P0} , ϵ , δ , θ , and ν :

$$V_G = f_2(V_{P0}, \epsilon, \delta, \tilde{\theta}, \nu). \quad (7)$$

The P-wave group angle ψ with the symmetry axis is also controlled by the angle-dependent phase velocity (e.g., Tsvankin, 2005):

$$\tan \psi = \frac{\tan \theta + \frac{1}{V} \frac{dV}{d\theta}}{1 - \frac{\tan \theta}{V} \frac{dV}{d\theta}}. \quad (8)$$

Hence, the angle $\tilde{\psi}$ with the vertical in a TTI layer can be written as

$$\tilde{\psi} = f_3(V_{P0}, \epsilon, \delta, \tilde{\theta}, \nu). \quad (9)$$

For the zero-offset reflection, the phase angle $\tilde{\theta} = \phi_b$ (Figure 3a), so

$$V_{G0} = f_2(V_{P0}, \epsilon, \delta, \phi_b, \nu), \quad (10)$$

and the group angle with the vertical is

$$\tilde{\psi}_0 = f_3(V_{P0}, \epsilon, \delta, \phi_b, \nu). \quad (11)$$

The length of the zero-offset raypath (AB in Figure 3a) can be calculated from the vertical thickness z_b of the layer measured in the borehole and the angles ϕ_b and $\tilde{\psi}_0$ (Figure 3a). AB can also be expressed through the two-way zero-offset reflection time t_0 and the group velocity given by equation 10:

$$\frac{z_b \cos \phi_b}{\cos(\tilde{\psi}_0 - \phi_b)} = \frac{V_{G0} t_0}{2}, \quad (12)$$

$\tilde{\psi}_0$ is found from equation 11. Note that if the CMP is displaced from the well by a known distance, equation 12 can be modified accordingly. Hence, we have constructed two equations (5 and 12) for the four unknown parameters.

We assume that the check-shot ray is vertical (i.e., its group angle with the vertical is zero), but the corresponding phase angle $\tilde{\theta}_{cs}$ is unknown (Figure 3b; the subscript “cs” denotes check-shot). Applying equations 7 and 9 to the vertical ray gives

$$f_2(V_{P0}, \epsilon, \delta, \tilde{\theta}_{cs}, \nu) = V_{G,cs}, \quad (13)$$

$$f_3(V_{P0}, \epsilon, \delta, \tilde{\theta}_{cs}, \nu) = 0. \quad (14)$$

The pure-mode NMO velocity for 2D wave propagation in a vertical symmetry plane of a homogeneous layer can be obtained as the following function of the phase velocity $V(\theta)$ and reflector dip ϕ (Tsvankin, 2005):

$$V_{nmo}(\phi) = \frac{V(\phi)}{\cos \phi} \frac{\sqrt{1 + \frac{1}{V(\phi)} \frac{d^2 V}{d\theta^2}}}{1 - \frac{\tan \phi}{V(\phi)} \frac{dV}{d\theta}} \Bigg|_{\theta=\phi}. \quad (15)$$

In a dipping TTI layer (Figure 3), the phase velocity and its derivatives in equation 15 should be computed at the phase angle $\theta_0 = \phi_b - \nu$ with the symmetry axis. Alternatively, it is possible to obtain V_{nmo} as a function of the known reflection slope p . Therefore, equation 15 yields another constraint on the medium parameters:

$$V_{nmo} = f_4(V_{P0}, \epsilon, \delta, \phi_b, \nu). \quad (16)$$

Therefore, the input data provide five equations (5, 12–14, and 16)

to be inverted for the four TTI parameters ($V_{P0}, \epsilon, \delta, \nu$) and the phase angle $\tilde{\theta}_{cs}$ corresponding to the check-shot ray:

$$f_1(V_{P0}, \epsilon, \delta, \phi_b, \nu) = \frac{\sin \phi_b}{p}; \quad (17)$$

$$f_2(V_{P0}, \epsilon, \delta, \phi_b, \nu) \cos[f_3(V_{P0}, \epsilon, \delta, \phi_b, \nu) - \phi_b] = \frac{2z_b \cos \phi_b}{t_0}; \quad (18)$$

$$f_2(V_{P0}, \epsilon, \delta, \tilde{\theta}_{cs}, \nu) = V_{G,cs}; \quad (19)$$

$$f_3(V_{P0}, \epsilon, \delta, \tilde{\theta}_{cs}, \nu) = 0; \quad (20)$$

$$f_4(V_{P0}, \epsilon, \delta, \phi_b, \nu) = V_{nmo}. \quad (21)$$

For VTI media (i.e., $\nu = 0^\circ$), V_{P0} is obtained directly from check shots because for a vertical borehole $V_{P0} = V_{G,cs}$; then ϵ and δ are found from equations 17 and 21. Even if the dip is unknown, the parameters ϵ , δ , and ϕ_b can be estimated from equations 17, 18, and 21. Here, however, we concentrate on the inversion for a nonzero tilt ν .

Synthetic example

Although the number of equations is equal to the number of unknowns, equations 17–21 form a nonlinear system, which is not guaranteed to have a unique solution. To evaluate the feasibility of the inversion, we computed the input data (p, t_0, V_{nmo} , and $V_{G,cs}$) from the exact equations and contaminated them by Gaussian noise with the standard deviations equal to 1% for p and t_0 , and 2% for V_{nmo} and $V_{G,cs}$. The reflector dip ϕ_b and depth z_b were assumed to be known exactly, and the starting model was isotropic (i.e., $\epsilon = \delta = 0$). Table 1 shows the inversion results for typical TTI parameters using 100 realizations of the input data. Despite the borehole constraints, the inversion proves to be highly unstable, with small errors in the data producing large distortions in the estimated parameters. This instability is partially caused by the nonlinear dependence of the phase

Table 1. Actual and estimated parameters of a homogeneous TTI layer. The dip and depth of the reflector are assumed to be known. The input data are contaminated by Gaussian noise with the standard deviations equal to 1% for p and t_0 , and 2% for V_{nmo} and $V_{G,cs}$. The mean values and standard deviations of the inverted parameters are denoted by “mean” and “sd,” respectively.

	Actual	Estimated	
		mean	sd
V_{P0} (km/s)	2.50	2.92	0.25
ϵ	0.25	0.15	0.77
δ	0.10	−0.14	0.14
ν (°)	50	−20	33
Dip ϕ_b (°)	30	—	—
Depth z_b (km)	1	—	—

velocity V on the tilt ν (Grechka et al., 2002a). Similar results were obtained for a wide range of model parameters.

Symmetry axis orthogonal to the reflector

If TTI symmetry is associated with dipping shale layers, the symmetry axis is typically assumed to be orthogonal to the layer boundaries (Isaac and Lawton, 1999; Vestrum et al., 1999; Charles et al., 2008). Fixing the orientation of the symmetry axis helps mitigate the nonuniqueness of the inversion procedure (Grechka et al., 2002a; Zhou et al., 2008; Behera and Tsvankin, 2009).

Inversion methodology

If the symmetry axis is orthogonal to the reflector, the tilt ν is equal to the reflector dip ϕ_b measured in the borehole. Also, the phase-velocity vector of the zero-offset reflection is parallel to the symmetry axis, and the velocity V_{P0} can be obtained directly from surface data and the dip ϕ_b (equation 17):

$$V_{P0} = \frac{\sin \phi_b}{p}. \quad (22)$$

The NMO velocity (equation 21) for $\nu = \phi_b$ is given by the isotropic cosine-of-dip relationship (Tsvankin, 2005):

$$V_{nmo} = \frac{V_{nmo}(0)}{\cos \phi_b}, \quad (23)$$

where $V_{nmo}(0) = V_{P0} \sqrt{1 + 2\delta}$. Since V_{P0} is already known, equation 23 constrains the parameter δ .

Because the group and phase velocities in the symmetry direction coincide, equation 18 includes only known quantities and can be used to check the validity of the model. Therefore, the inverse problem reduces to estimating the parameters ϵ and $\tilde{\theta}_{cs}$ from the vertical group velocity (i.e., from equations 19 and 20):

$$f_2(V_{P0}, \epsilon, \delta, \tilde{\theta}_{cs}, \phi_b) = V_{G,cs}; \quad (24)$$

$$f_3(V_{P0}, \epsilon, \delta, \tilde{\theta}_{cs}, \phi_b) = 0. \quad (25)$$

When $\nu = \phi_b$, the inversion equations do not include z_b and are independent of the CMP location. Moreover, if the check-shot ray is not exactly vertical but its inclination is known, equations 24 and 25 retain the same form with a nonzero group angle on the right-hand side of equation 25.

Synthetic examples

First, we perform a test on noise-contaminated data for a model with $\nu = \phi_b = 30^\circ$ and typical values of the Thomsen parameters (Figure 4a). The parameters V_{P0} and δ can be estimated with high accuracy because they are well constrained by our data; the mean value of V_{P0} is 2.50 km/s with the standard deviation 1%; the mean value of δ is 0.10 with the standard deviation 0.03. However, the parameter ϵ is practically unconstrained (the standard deviation is 1.37). The instability in estimating ϵ can be explained using the linearized weak-anisotropy approximation. For weak anisotropy, the magnitudes of the phase- and group-velocity vectors coincide (Thomsen, 1986), and for the vertical ray

$$V_{G,cs} = V_{p0}(1 + \delta \sin^2 \phi_b \cos^2 \phi_b + \epsilon \sin^4 \phi_b). \quad (26)$$

For moderate dips, such as $\phi_b = 30^\circ$ used in the test, the contribution of ϵ to $V_{G,cs}$ is much smaller than that of δ because ϵ is multiplied with $\sin^4 \phi_b$. As a result, the objective function has multiple local minima for ϵ that hamper the convergence of the algorithm.

The estimates of V_{p0} and δ are sufficiently accurate for a wide range of dips, with small (and practically constant) standard deviations (Table 2). The errors in the parameter ϵ , however, are much larger; to resolve ϵ from the vertical group velocity, the dip (and tilt) should reach at least 60° . Note that our algorithm operates with NMO velocity, which controls reflection moveout for offset-to-depth ratios limited by unity. If long-spread P-wave data (with the offset-to-depth ratio reaching two) are available, it is possible to estimate ϵ from nonhyperbolic moveout analysis (Behera and Tsvanin, 2009).

When the symmetry axis is not orthogonal to the reflector, the algorithm based on setting $\nu = \phi_b$ produces errors in the inverted parameters. However, for typical moderate magnitudes of ϵ and δ ($|\epsilon| \leq 0.5$; $|\delta| \leq 0.3$), the errors in V_{p0} and δ remain small, if the symmetry axis deviates from the reflector normal by less than 5° and the dip ranges from 5° to 50° (Table 3). For example, we computed the input data with the actual tilt $\nu = 15^\circ$ and dip $\phi_b = 20^\circ$, then obtained the parameters $V_{p0} = 2.5$ km/s and $\delta = 0.11$ under the assumption that $\nu = \phi_b = 20^\circ$. The inversion results become more distorted for strong anisotropy and/or large dips because the value of $(\sin \phi_b / p)$ differs more significantly from the actual symmetry-direction velocity V_{p0} , and the errors are amplified in the inversion of the NMO velocity for δ .

INVERSION FOR LAYERED TTI MEDIA

In the previous section we demonstrated the feasibility of 2D inversion of P-wave moveout and borehole measurements for the parameters of a single TTI layer with the symmetry axis orthogonal to its bottom. Here, we present an algorithm for interval parameter estimation in layered TTI media using reflection and borehole data.

The model is composed of homogeneous TTI layers separated by plane dipping boundaries with the same azimuth of the dip plane.

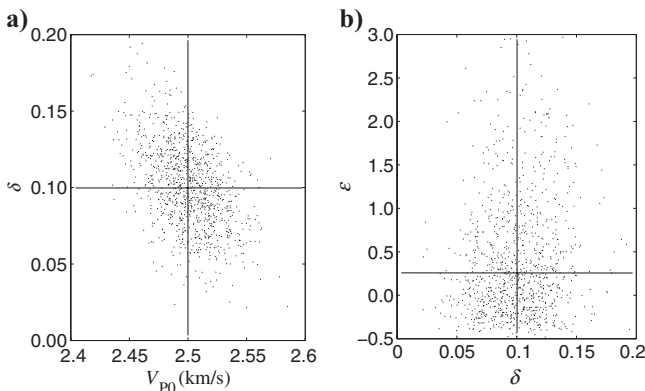


Figure 4. Inversion results (dots) for a TTI layer with the symmetry axis orthogonal to its bottom. The inversion was carried out for 1000 realizations of input data contaminated by Gaussian noise with the standard deviations equal to 1% for the reflection slope p and 2% for V_{nmo} and $V_{G,cs}$. Due to the large standard deviation (1.37) of ϵ , the vertical axis on plot (b) is clipped. The actual parameter values are marked by the crosses. The starting model was isotropic.

The symmetry axis in each layer is perpendicular to its bottom, which makes wave propagation two-dimensional. The model vector for an N -layered medium contains $3N$ unknowns:

$$\tilde{m} = \{V_{p0}^{(n)}, \epsilon^{(n)}, \delta^{(n)}\}, \quad (n = 1, 2, \dots, N). \quad (27)$$

The data vector has the form

$$\tilde{d} = \{t_0(n), p(n), V_{nmo}(n), z_b^{(n)}, \phi_b^{(n)}, t_{cs}(m)\}, \quad (n = 1, 2, \dots, N), \quad (m = 1, 2, \dots, M), \quad (28)$$

where $t_0(n)$, $p(n)$, and $V_{nmo}(n)$ are the effective values for the n th reflector measured from reflection data, $z_b^{(n)}$ and $\phi_b^{(n)}$ are the depth and dip of the n th reflector, respectively, at the borehole location, and $t_{cs}(m)$ is the check-shot traveltime for the m th receiver placed in the borehole. The tilt $\nu^{(n)}$ in each layer is equal to the dip $\phi_b^{(n)}$ of the layer's bottom.

Inversion methodology

This algorithm generalizes the inversion scheme for a single TTI layer discussed above, and it represents a modification of P-wave

Table 2. Inversion results for a TTI layer with the symmetry axis perpendicular to its bottom (i.e., the tilt is equal to the dip). The medium parameters are $V_{p0} = 2.50$ km/s, $\delta = 0.10$, and $\epsilon = 0.25$. The data are contaminated by Gaussian noise with the standard deviations equal to 1% for p , and 2% for V_{nmo} and $V_{G,cs}$.

Dip ϕ_b ($^\circ$)	V_{p0}		δ		ϵ	
	mean (km/s)	sd (%)	mean	sd	mean	sd
10	2.50	1	0.10	0.03	282	854
30	2.50	1	0.10	0.03	0.64	1.37
50	2.50	1	0.10	0.03	0.27	0.13
70	2.50	1	0.10	0.03	0.25	0.05

Table 3. Inverted values of δ for a TTI layer with the symmetry axis deviating from the reflector normal by $\pm 5^\circ$. The parameters V_{p0} and δ are obtained under the assumption that the symmetry axis is orthogonal to the reflector. The input data are contaminated by Gaussian noise with the standard deviations equal to 1% for p , and 2% for V_{nmo} and $V_{G,cs}$. The mean values of V_{p0} are close to 2.50 km/s, and the standard deviation to 1%.

Dip ϕ_b ($^\circ$)	ν ($^\circ$)	δ	
		mean	sd
5	0	0.11	0.03
5	10	0.10	0.03
20	15	0.11	0.03
20	25	0.10	0.03
40	35	0.12	0.03
40	45	0.09	0.03
60	55	0.15	0.03
60	65	0.07	0.03

stacking-velocity tomography introduced for VTI media by Grechka et al. (2002b). The model geometry can be fully reconstructed from the known depths and dips of the interfaces. Then for a trial set \tilde{m} of the interval parameters (equation 27), we trace the zero-offset ray from an arbitrary point on the n th reflector up to the surface. The slowness vector at the reflection point is perpendicular to the interface. Because the model is composed of homogeneous layers separated by plane interfaces, the zero-offset rays for different CMP locations have the same slowness vector in each layer. Therefore, the calculated horizontal slowness $p^{\text{calc}}(n)$ of the zero-offset ray at the surface can be used to fit the measurements $p(n)$. Then we trace the zero-offset ray downward from the source location using the slowness components computed in each layer (but with the opposite sign), and calculate the zero-offset traveltimes $t_0^{\text{calc}}(n)$. Also, the NMO velocities $V_{\text{nmo}}^{\text{calc}}(n)$ are obtained using the Dix-type averaging equations for piecewise-homogeneous media (Grechka et al., 2002b).

For check-shot data, we employ one receiver per layer located close to the layer's bottom so that the interval traveltime can be estimated with sufficient accuracy. Using the trial interval parameters and the known model geometry, we trace the check-shot ray for a specific receiver, which yields the traveltime $t_{\text{cs}}^{\text{calc}}(n)$. Note that check-shot data for multilayered media do not directly constrain the interval group velocity (equation 24). Fitting the traveltimes $t_{\text{cs}}(n)$ is equivalent to solving equations 24 and 25 for a single layer because the phase angle $\tilde{\theta}_{\text{cs}}$ for each ray is found from the trial medium parameters.

The interval parameters $\{V_{\text{p0}}^{(n)}, \epsilon^{(n)}, \delta^{(n)}\}$ are estimated by minimizing the objective function that contains the differences between the calculated and measured quantities:

$$\mathcal{F}(\tilde{m}) \equiv \sum_{n=1}^N \left(\frac{\|p^{\text{calc}}(n) - p(n)\|^2}{\sigma^2[p(n)]} + \frac{\|t_0^{\text{calc}}(n) - t_0(n)\|^2}{\sigma^2[t_0(n)]} + \frac{\|V_{\text{nmo}}^{\text{calc}}(n) - V_{\text{nmo}}(n)\|^2}{\sigma^2[V_{\text{nmo}}(n)]} + \frac{\|t_{\text{cs}}^{\text{calc}}(n) - t_{\text{cs}}(n)\|^2}{\sigma^2[t_{\text{cs}}(n)]} \right), \quad (29)$$

where σ^2 represents the variance of each measurement. Grechka et al. (2002b) fit only P-wave NMO ellipses in their objective function for VTI media, because their input data do not include borehole information. Our algorithm operates with 2D data, so we use a single NMO velocity instead of the three parameters of the NMO ellipse. However, we assume to know the model geometry and have check-shot traveltimes.

The depths $z_b^{(n)}$ and dips $\phi_b^{(n)}$ are not included in the objective function because they are used to compute the other quantities; also, the dip $\phi_b^{(n)}$ helps constrain the tilt $\nu^{(n)}$ of the symmetry axis in each layer. For a single layer, the parameter ϵ is obtained from the group velocity (equations 24 and 25). However, for layered TTI media, the interval parameter ϵ also contributes to $p(n)$, $t_0(n)$, and $V_{\text{nmo}}(n)$ (except for $n = 1$). Therefore, although $\epsilon^{(n)}$ is not expected to be well constrained, it has to be estimated together with $V_{\text{p0}}^{(n)}$ and $\delta^{(n)}$ using equation 29.

It should be emphasized that we invert for all interval parameters simultaneously without employing layer stripping. This feature of the algorithm helps mitigate error accumulation with depth and is particularly beneficial when the model includes a layer at depth that is known to be isotropic. Then, as demonstrated by Grechka et al. (2001) on physical-modeling data for a bending TTI thrust sheet, the reflection from the bottom of the isotropic layer provides valuable constraints on the parameters of the TTI overburden.

As the previous implementations of stacking-velocity tomography, our algorithm assumes each layer to be homogeneous. The influence of lateral velocity variation on the inversion results is expected to be relatively minor because the maximum offset of reflection data can be limited by the reflector depth. Ignoring the vertical velocity gradient between reflectors typically causes overestimation of the parameter δ (Grechka and Tsvankin, 2002a). The purpose of our algorithm, however, is to provide a simple tool for building an initial velocity model that can be refined using reflection tomography or other methods operating in the migrated domain (Woodward et al., 2008; Bakulin et al., 2009).

Synthetic example

The algorithm was tested on models with up to four TTI layers with dips ranging from 0° to 60° and the anisotropy parameters varying within the plausible range (from zero to 0.5 for ϵ and from -0.2 to 0.3 for δ). The results of a typical test for a three-layer medium (Figure 5 and Table 4) are shown in Figure 6. The inversion is performed for 200 realizations of noise-contaminated input data using the value of each measurement as its variance σ^2 in equation 29. Since the dips are moderate, estimation of the interval parameter ϵ is unstable, while V_{p0} and δ can be recovered with sufficiently high accuracy. The standard deviations of the estimated parameters are higher in the third layer (about 3% for V_{p0} and 0.06 for δ). This reduction in accuracy is related primarily to the smaller contribution of the deeper layers to the effective reflection traveltimes. Our tests in-

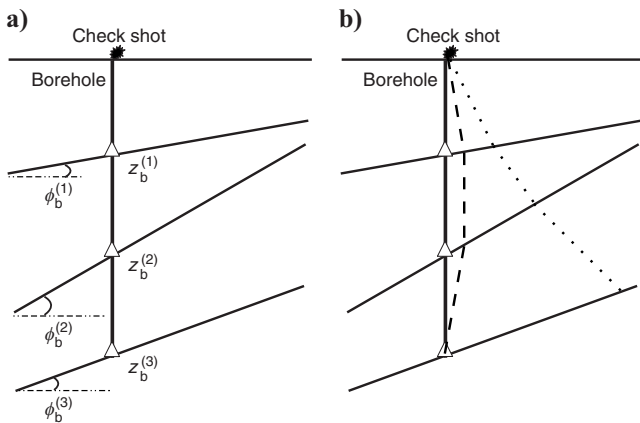


Figure 5. Three-layer TTI model used to test the inversion algorithm. The input data for parameter estimation are computed by anisotropic ray tracing. (a) The dips are $\phi_b^{(1)} = 10^\circ$, $\phi_b^{(2)} = 30^\circ$, and $\phi_b^{(3)} = 20^\circ$. The reflector depths at the borehole location are $z_b^{(1)} = 1$ km, $z_b^{(2)} = 2$ km, and $z_b^{(3)} = 3$ km. The check-shot source is located 10 m to the right of the borehole; the receivers (marked by triangles) are placed at the intersection of the borehole with each reflector. (b) The check-shot (dashed) and zero-offset (dotted) rays for the third reflector.

dicating that the thickness-to-depth ratio of a layer at the borehole location should be at least 25% to ensure reliable estimation of the interval parameters.

If the maximum difference between the reflector dips exceeds 30°, the errors in the interval parameter δ rapidly increase for the deeper layers. This happens mainly because the zero-offset and check-shot traveltimes depend not only on the interval parameters V_{p0} and δ , but also on the values of ϵ in the overburden. This influence of the interval ϵ becomes more significant for models with a wide range of dips. Since ϵ is not well constrained by the input data, its contribution to the objective function increases errors in δ .

INVERSION WITHOUT DIP INFORMATION

If accurate dip measurements are not available, it may still be possible to obtain stable estimates of V_{p0} and δ , as well as of the dip itself. In a single TTI layer with the symmetry axis orthogonal to its bottom, V_{p0} cannot be obtained from the time slope p if the dip ϕ (here we do not use the subscript “b”) is unknown (equation 22). However, the reflector depth z_b measured in the borehole provides a second relationship between V_{p0} and ϕ :

$$z_b = \frac{t_0 V_{p0}}{2 \cos \phi}. \tag{30}$$

Equation 30 represents a simplified form (valid for $\nu = \phi$) of equation 18. Equations 22 and 30 can be solved for V_{p0} and ϕ , which allows us to find δ from the NMO velocity (equation 23). Synthetic

Table 4. Interval parameters of the three-layer TTI model from Figure 5. The symmetry axis in each layer is orthogonal to its lower boundary. The input data are distorted by Gaussian noise with the standard deviations equal to 1% for $p(n)$, $t_0(n)$, and $t_{cs}(n)$, and 2% for V_{nmo} .

	Layer 1	Layer 2	Layer 3
V_{p0} (km/s)	1.5	2.0	2.5
ϵ	0.10	0.20	0.25
δ	-0.10	0.10	0.12
ν (°)	10	30	20

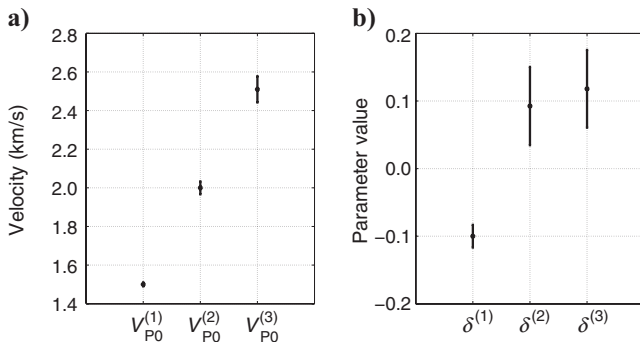


Figure 6. (a) Interval symmetry-direction velocities $V_{p0}^{(n)}$ and (b) anisotropy parameters $\delta^{(n)}$ ($n = 1, 2, 3$) estimated by our algorithm for the model from Figure 5 and Table 4. The dots mark the mean values, and the bars correspond to the \pm standard deviation in each parameter.

tests confirm that our algorithm yields accurate values of the parameters V_{p0} , δ , and ϕ for a single layer.

However, estimation of the interval parameters V_{p0} and δ for layered TTI models with unknown interface dips requires additional information. One practical option is to include walkaway vertical seismic profiling (VSP) traveltimes to increase the angle coverage of the input data. Extensive numerical testing shows that it is sufficient to add two VSP sources placed on both sides of the borehole at a distance that reaches at least 1/5 of the largest reflector depth. We reproduced the test for the model in Figure 5 and Table 4 with the input data vector (see equation 28) that did not include the dip information. Instead, we added the noise-contaminated VSP traveltimes (t_{VSP}) for two sources located ± 0.6 km to the left and right of the borehole, so that the input data were comprised of V_{nmo} , p , t_0 , t_{cs} , and t_{VSP} . The results are similar to those in Figure 6, with the standard deviation of the interval δ -values changing by less than 0.01.

To simulate an overthrust structure typical for such areas as the Canadian Foothills, we construct a model that includes a TTI layer with parallel dipping boundaries embedded in a homogeneous, isotropic background (Figure 7; the dip is 50°). The inversion for the interval parameters V_{p0} , δ , ϵ , and ϕ is carried out under the assumption that each layer is TTI with the symmetry axis orthogonal to its lower boundary. The algorithm is applied to 200 realizations of noise-contaminated input data with the standard deviations equal to 2% for V_{nmo} , and 1% for p , t_0 , t_{cs} , and t_{VSP} . The mean values of V_{p0} , δ , and ϕ for the TTI layer are close to the actual parameters, while the standard deviations are 4%, 0.04, and 0.6°, respectively. Since the dip is relatively large, even the interval parameter ϵ in this model is

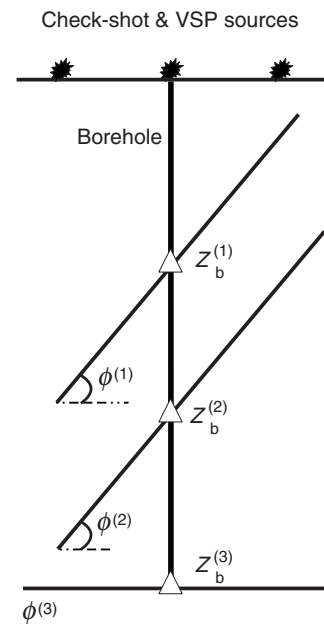


Figure 7. Dipping TTI layer with parallel boundaries embedded in isotropic host rock. The known reflector depths at the borehole location are $z_b^{(1)} = 1$ km, $z_b^{(2)} = 1.7$ km, and $z_b^{(3)} = 2.5$ km. The dips (assumed to be unknown) are $\phi^{(1)} = 50^\circ$, $\phi^{(2)} = 50^\circ$, and $\phi^{(3)} = 0^\circ$. The check-shot source is located 10 m to the right of the borehole; two additional VSP sources are ± 500 m away from the borehole. The receivers (marked by triangles) are placed at the intersection of the borehole with each reflector. The parameters of the TTI layer are $V_{p0} = 2.9$ km/s, $\delta = 0.08$, $\epsilon = 0.16$, and $\nu = \phi = 50^\circ$. The velocity in the isotropic background is 2.7 km/s.

well-constrained (the mean value is 0.18, the standard deviation is 0.05).

DISCUSSION AND CONCLUSIONS

P-wave reflection traveltimes typically do not contain enough information for estimating the full parameter set of tilted TI models and performing depth imaging. Here, we presented a 2D inversion algorithm for TTI media that supplements P-wave NMO velocities, zero-offset traveltimes, and reflection time slopes with borehole data. It was assumed that borehole measurements include check-shot traveltimes along with the depths and dips of layer boundaries.

The inversion for a single TTI layer above a dipping reflector (the symmetry axis is confined to dip plane) was based on exact expressions for the phase, group, and NMO velocities. Although the input data allow us to construct enough equations for the symmetry-direction velocity V_{p0} , anisotropy parameters ϵ and δ , and the tilt ν of the symmetry axis, synthetic tests proved the inversion procedure to be highly unstable. Since this problem is caused primarily by an unknown tilt ν , we fixed the symmetry axis in the direction orthogonal to the reflector. This common constraint makes it possible to obtain the parameters V_{p0} and δ with high accuracy for the full range of reflector dips. However, the parameter ϵ still cannot be resolved for dips (and tilts) under 60° because its estimation requires large propagation angles with the symmetry axis. If the magnitude of anisotropy is not uncommonly large ($|\epsilon| \leq 0.5$; $|\delta| \leq 0.3$) and the dip does not exceed 50° , the algorithm can tolerate the deviation of the symmetry axis from the reflector normal by $\pm 5^\circ$.

To perform interval parameter estimation for a stack of TTI layers separated by plane dipping interfaces, we employed a tomographic-style algorithm that operates with conventional-spread P-wave moveout. The current implementation is limited to the 2D model, in which the vertical incidence plane coincides with the dip planes of all interfaces, and the symmetry axis in each layer is perpendicular to its bottom. The depths and dips of the reflectors are assumed to be measured in the borehole, which allows us to reconstruct the model geometry. The objective function, computed by ray tracing using trial interval parameters, includes the time slope, zero-offset traveltimes, and NMO velocity of each reflection event along with check-shot traveltimes. By performing the inversion for all layers simultaneously, the algorithm mitigates error accumulation with depth. Testing on noise-contaminated data showed that for models with the maximum difference between reflector dips not exceeding 30° , the interval V_{p0} and δ are well-resolved. If long-spread P-wave data are available, ϵ can be obtained from nonhyperbolic moveout inversion.

When accurate dip information is unavailable, it can be replaced by traveltimes for at least two VSP sources placed on both sides of the borehole. If the distance between each VSP source and the borehole reaches $1/5$ of the largest reflector depth, the algorithm produces stable estimates of V_{p0} , δ , and the reflector dips.

Our method can be extended in a straightforward way to 3D wide-azimuth P-wave data by including the NMO ellipses in the objective function. Under the same assumption as in 2D case (i.e., the symmetry axis in each layer is orthogonal to its bottom), wide-azimuth data provide additional information for estimating the interval Thomsen parameters. As will be shown in a sequel paper, the interval parameters V_{p0} and δ along with the reflector dips and azimuths can be resolved from 3D stacking-velocity inversion with only one borehole

constraint — the depth of each reflector (no check-shot or walkaway VSP data are needed).

Stacking-velocity tomography, possibly supplemented with non-hyperbolic moveout inversion for ϵ , represents an efficient tool for building an initial model for migration velocity analysis (MVA) and postmigration reflection tomography. After carrying out the interval parameter estimation at well locations, the V_{p0} - and δ -fields can be computed by interpolation between the wells. An accurate initial TTI model is critically important to ensure the convergence of MVA-based algorithms.

ACKNOWLEDGMENTS

We are grateful to Andrey Bakulin (WesternGeco), Paul Fowler (WesternGeco), Vladimir Grechka (Shell), and Andres Pech (IPN, Mexico) for making available their codes and numerous helpful suggestions. We also thank Andrey Bakulin, Brian Macy (ConocoPhillips), and two anonymous referees for their reviews of the manuscript and our colleagues at the Center for Wave Phenomena (CWP) for valuable discussions and technical assistance. This work was supported by the Consortium Project on Seismic Inverse Methods for Complex Structures at CWP.

REFERENCES

- Alkhalifah, T., and K. Larner, 1994, Migration error in transversely isotropic media: *Geophysics*, **59**, 1405–1418.
- Alkhalifah, T., I. Tsvankin, K. Larner, and J. Toldi, 1996, Velocity analysis and imaging in transversely isotropic media: Methodology and a case study: *The Leading Edge*, **15**, 371–378.
- Bakulin, A., M. Woodward, D. Nichols, K. Osypov, and O. Zdraveva, 2009, Building TTI depth models using anisotropic tomography with well information: 79th Annual International Meeting, SEG, Expanded Abstracts, 4029–4033.
- Behera, L., and I. Tsvankin, 2009, Migration velocity analysis for tilted TI media: *Geophysical Prospecting*, **57**, 13–26.
- Charles, S., D. R. Mitchell, R. A. Holt, J. Lin, and J. Mathewson, 2008, Data-driven tomographic velocity analysis in tilted transversely isotropic media: A 3D case history from the Canadian Foothills: *Geophysics*, **73**, no. 5, VE261–VE268.
- Dewangan, P., and I. Tsvankin, 2006a, Modeling and inversion of PS-wave moveout asymmetry for tilted TI media: Part I — Horizontal TTI layer: *Geophysics*, **71**, no. 4, D107–D121.
- , 2006b, Modeling and inversion of PS-wave moveout asymmetry for tilted TI media: Part II — Dipping TTI layer: *Geophysics*, **71**, no. 4, D123–D134.
- Grechka, V., and P. Dewangan, 2003, Generation and processing of pseudo-shear-wave data: Theory and case study: *Geophysics*, **68**, 1807–1816.
- Grechka, V., A. Pech, and I. Tsvankin, 2002a, Multicomponent stacking-velocity tomography for transversely isotropic media: *Geophysics*, **67**, 1564–1574.
- , 2002b, P-wave stacking-velocity tomography for VTI media: *Geophysical Prospecting*, **50**, 151–168.
- Grechka, V., A. Pech, I. Tsvankin, and B. Han, 2001, Velocity analysis for tilted transversely isotropic media: A physical-modeling example: *Geophysics*, **66**, 904–910.
- Grechka, V., and I. Tsvankin, 2000, Inversion of azimuthally dependent NMO velocity in transversely isotropic media with a tilted axis of symmetry: *Geophysics*, **65**, 232–246.
- , 2002a, Processing-induced anisotropy: *Geophysics*, **67**, 1920–1928.
- , 2002b, PP + PS = SS: *Geophysics*, **67**, 1961–1971.
- Huang, T., S. Xu, J. Wang, G. Ionescu, and M. Richardson, 2008, The benefit of TTI tomography for dual azimuth data in Gulf of Mexico: 78th Annual International Meeting, SEG, Expanded Abstracts, 222–226.
- Isaac, J. H., and D. C. Lawton, 1999, Image mispositioning due to dipping TI media: A physical seismic modeling study: *Geophysics*, **64**, 1230–1238.
- Sexton, P., and P. Williamson, 1998, 3D anisotropic velocity estimation by model-based inversion of pre-stack traveltimes: 68th Annual International Meeting, SEG, Expanded Abstracts, 1855–1858.
- Thomsen, L., 1986, Weak elastic anisotropy: *Geophysics*, **51**, 1954–1966.
- Tsvankin, I., 1996, P-wave signatures and notation for transversely isotropic media: An overview: *Geophysics*, **61**, 467–483.

- , 2005, *Seismic signatures and analysis of reflection data in anisotropic media*, 2nd ed.: Elsevier Science.
- Tsvankin, I., and V. Grechka, 2000, Dip moveout of converted waves and parameter estimation in transversely isotropic media: *Geophysical Prospecting*, **48**, 257–292.
- Vestrum, R. W., D. C. Lawton, and R. Schmid, 1999, Imaging structures below dipping TI media: *Geophysics*, **64**, 1239–1246.
- Woodward, M. J., D. Nichols, O. Zdraveva, P. Whitfield, and T. Johns, 2008, A decade of tomography: *Geophysics*, **73**, no. 5, VE5–VE11.
- Zhou, B., S. Greenhalgh, and A. Green, 2008, Nonlinear travelttime inversion scheme for crosshole seismic tomography in tilted transversely isotropic media: *Geophysics*, **73**, no. 4, D17–D33.